Assessment of Analytical Methods Used to Predict the Structural Response of 12-inch Concrete Substantial Dividing Walls to Blast Loading

David D. Bogosian, P. E.
Karagozian & Case Structural Engineers
625 N. Maryland Avenue
Glendale, CA 91206-2245

William H. Zehrt, Jr., P. E.
U. S. Army Engineering and Support Center, Huntsville
P. O. Box 1600
Huntsville, AL 35807-4301

ABSTRACT: When 12-inch concrete substantial dividing walls are used to protect personnel from explosive effects, the typical allowable explosive weight, when calculated using the methods in Army TM 5-1300, is less than 2 pounds TNT. Comparison of results from state-of-the-art nonlinear finite element models to actual data from accidental explosions shows that even well validated, high fidelity, physics-based analytical methods grossly overpredict the response of these walls. Consideration of the observed damage from these accidents indicates that mothodology used to compute the gas pressure portion of the blast loads incorporates significant levels of conservatism. Further analytical and experimental investigation to reduce this level of conservatism could allow up to an order of magnitude increase in the allowable net explosive weight for personnel protection.

INTRODUCTION

Within the U. S. Department of Defense (DoD), barriers which are effective in subdividing ammunition and explosives are defined as “substantial dividing walls” (SDWs). Over the years, a standard design for these SDWs has evolved consisting of a 12-inch thick concrete wall with 2 layers of ½-inch diameter (#4) vertical and horizontal steel bars at a spacing of 12 inches on center. One bar layer is placed at each face of the wall, with the bars in each layer staggered between the two faces. A minimum concrete compressive strength of 2,500 psi is prescribed. The strength of the steel reinforcement tends to vary with the age of the structure: older SDWs use grade 40 steel (40 ksi yield strength) while newer ones use grade 60 (60 ksi yield).

Large numbers of SDWs exist throughout the munitions production, operations, maintenance, and storage infrastructure. Since World War II, they have been used as operational shields for personnel, providing protection from the accidental detonation of up to 15 pounds of Hazard Division 1.1 explosives.

In the DoD Ammunition and Explosives Safety Standards [1], Army Technical Manual 5-1300 [2] is referenced for the design of suitable barriers, such as dividing walls, to provide protection from blast effects. For protection of personnel, the safety standard limits the allowable exposure to blast effects, thereby providing personnel with a high degree of protection from serious injury. Using TM 5-1300, explosive limits for 12-inch concrete SDWs will vary depending upon numerous parameters including charge location, cubicle dimensions, dividing wall support conditions, and frangibility of other structural elements. Typically, however, the maximum

Report Documentation Page

Form Approved
OMB No. 0704-0188

1. REPORT DATE **AUG 1998**	2. REPORT TYPE	3. DATES COVERED **00-00-1998 to 00-00-1998**

4. TITLE AND SUBTITLE **Assessment of Analytical Methods Used to Predict the Structural Response of 12-inch Concrete Substantial Dividing Walls to Blast Loading**	5a. CONTRACT NUMBER 5b. GRANT NUMBER 5c. PROGRAM ELEMENT NUMBER
6. AUTHOR(S)	5d. PROJECT NUMBER 5e. TASK NUMBER 5f. WORK UNIT NUMBER
7. PERFORMING ORGANIZATION NAME(S) AND ADDRESS(ES) **U. S. Army Engineering and Support Center, Huntsville,P. O. Box 1600,Huntsville,AL,35807-4301**	8. PERFORMING ORGANIZATION REPORT NUMBER
9. SPONSORING/MONITORING AGENCY NAME(S) AND ADDRESS(ES)	10. SPONSOR/MONITOR'S ACRONYM(S) 11. SPONSOR/MONITOR'S REPORT NUMBER(S)

12. DISTRIBUTION/AVAILABILITY STATEMENT
Approved for public release; distribution unlimited

13. SUPPLEMENTARY NOTES
See also ADM001002. Proceedings of the Twenty-Eighth DoD Explosives Safety Seminar Held in Orlando, FL on 18-20 August 1998.

14. ABSTRACT
see report

15. SUBJECT TERMS

16. SECURITY CLASSIFICATION OF:			17. LIMITATION OF ABSTRACT	18. NUMBER OF PAGES	19a. NAME OF RESPONSIBLE PERSON
a. REPORT **unclassified**	b. ABSTRACT **unclassified**	c. THIS PAGE **unclassified**	**Same as Report (SAR)**	**14**	

allowable net explosive weight for personnel protection calculated using these methods will be less than 2 pounds.

In an effort to investigate the degree of conservatism incorporated in the analytical methods of the TM 5-1300, the U. S. Army Industrial Operations Command, Safety Office funded a study to investigate the blast capacity of typical 12-inch concrete SDWs using more sophisticated nonlinear finite element modeling techniques, since the 2-pound criteria were widely regarded as being excessively low. The *a priori* assumption was that use of a more detailed model (i.e., finite element instead of single degree of freedom) would eliminate most of the conservatism and produce more realistic results. In order to validate the finite element models to be used in this study, an extensive literature search was conducted of the Department of Defense Explosives Safety Board (DDESB) and U. S. Army Technical Center for Explosives Safety (USATCES) accident files, as a result of which damage data were obtained from numerous accidents in which SDWs had been subjected to blast loads. Two particular accidents were isolated for detailed analytical investigation, the results of which are discussed below.

Subsequent to the validation analyses, a series of parametric analyses were also performed using similar finite element models [3], more or less confirming the low (i.e., less than 2 pounds) allowable explosive weights for the typical configuration obtained with TM 5-1300. The purpose of this paper, however, is to highlight the results of the validation study and to explore the implications of that study for the ways in which the loading, particularly the gas pressure phase, is calculated as part of the design and analysis process.

HISTORICAL ACCIDENT DATA

The first accident to be analyzed (designated V-1 herein) involved a total of about 7 lbs of PBX explosive with an approximate TNT equivalence of 8 lbs. A floor plan of the cubicle in which the the explosion occurred is shown in Figure 1: the cubicle measured 7'-6" in width by 9'-6" in depth, with concrete SDWs on three sides; the fourth frangible side was constructed of hollow clay tile blocks and had a personnel door in it. Immediately outside the frangible wall was a hallway beyond which was the exterior wall (frangible wood stud construction with large windows). The exact location of the charge at the time of the accident is not precisely known; for the purpose of these analyses it was assumed to be located at the plan center of the bay at a height of 3 feet above the floor.

A view of the damaged cubicle post-explosion is shown in Figure 2, in which the deformation of the SDW on the left is clearly visible along its top surface. The wall is bowed outward due to the pressure from within, a deformation that appears to be roughly on the order of 4 to 6 inches (using the 12-inch wall thickness for scaling). The wall on the right is also slightly deformed, but to a much lesser extent. The roof and front wall have completely disintegrated, scattering debris throughout the general vicinity of the room. In Figure 3 we see a close-up of the rear left corner, viewed from behind the cubicle, where the side wall cracked and separated from the back wall, a clear gap that appears to be roughly 3-4 inches wide. While the exact vertical location of the break is hard to pinpoint, it appears to have spread from near the bottom joint up to about 6 or 7 feet in height. The internal reinforcing bars are clearly visible and many of them are broken. Nevertheless, the wall remained standing and did not fail catastrophically, probably due to the restraining effect of the unbroken rebar at the higher elevations which provided integrity to the overall system by tying the top of the SDW to the perpendicular back wall.

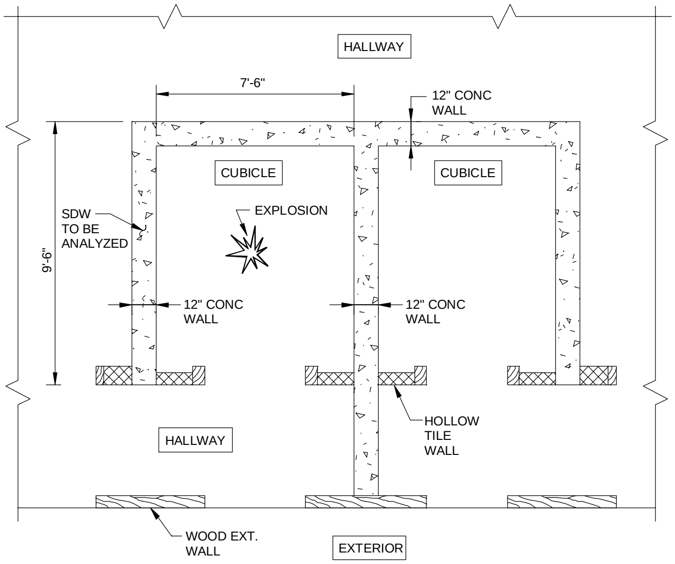

Figure 1. Plan view of cubicle for validation case V-1.

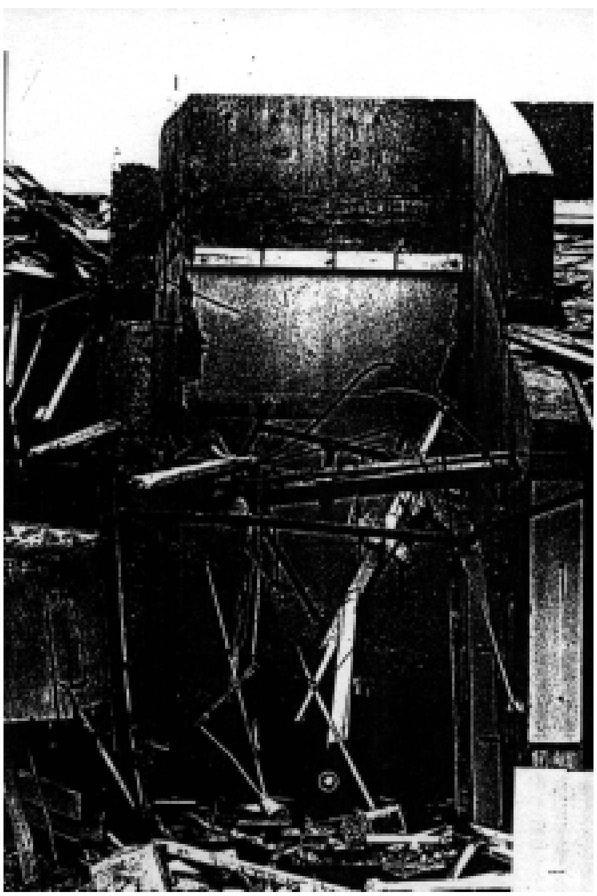

Figure 2. View of damaged cubicle.

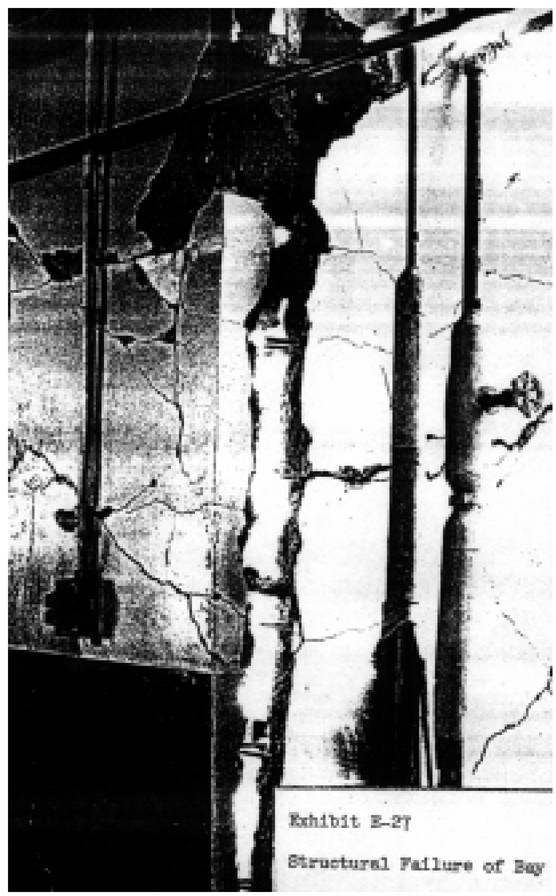

Figure 3. Close-up showing wall separation.

The second validation case (designated V-2) involved a cubicle similar to the first one but with somewhat different dimensions, as illustrated in Figure 4. The roof construction was of wood framing, while the frangible front wall (in this case venting directly to the exterior rather than to a corridor) was of hollow tile. The nature of the explosion in this case is somewhat more murky than in case V-1 because, at the time of the explosion, the room contained various amounts of various kinds of explosives, not all of which detonated. The best estimate of the charge size was that it ranged somewhere between 14 and 18 lb of TNT equivalence; hence, the analysis was run using a 16 lb charge weight, once again assumed to be in the center of the room. at a height of 3 feet above the floor.

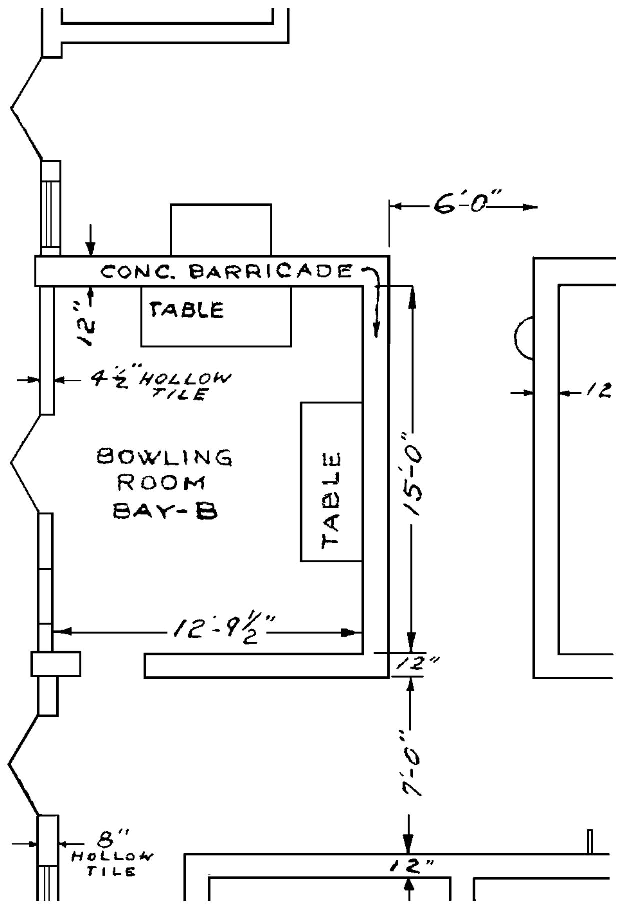

Figure 4. Plan view of cubicle used for validation case V-2.

A photograph of the post-detonation condition of the cubicle is shown in Figure 5. The entire roof over the cubicle has been blown away, with the exception of a strip overhanging the front of the building. The entire front wall has also been obliterated, and the adjacent area is strewn with roof and wall debris. The concrete side and back walls, however, are relatively intact with no visible deformation and no other significant damage. While some cracking of the concrete is quite likely to have occurred, none was apparently severe enough to warrant documentation as none of the post-event photographs record any kind of structural damage such as severe spallation, large cracks, or broken reinforcing.

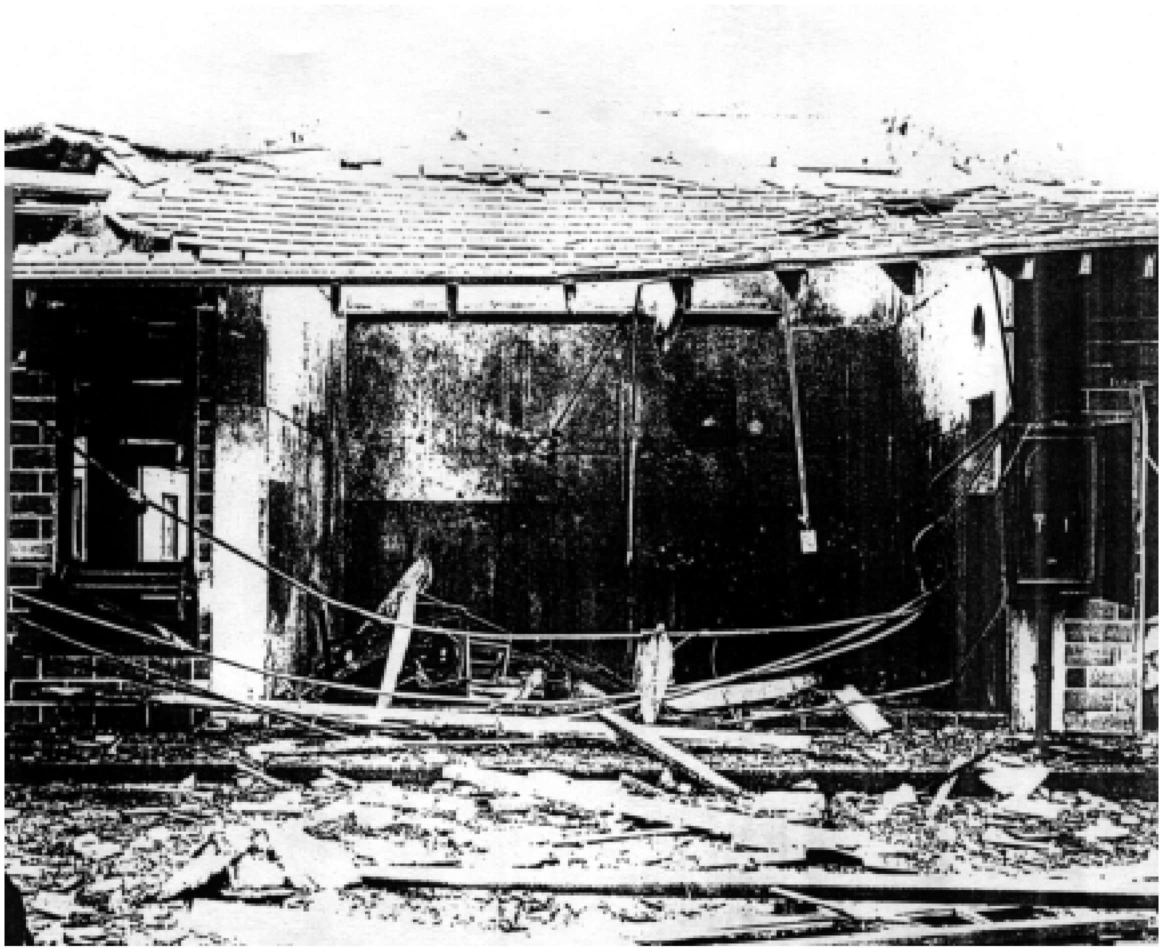

Figure 5. Post-accident view of damaged cubicle for case V-2

ANALYTICAL METHOD

The structural response calculations were performed using the DYNA3D explicit nonlinear finite element code [4]. The code is well adapted to solving dynamic nonlinear problems involving structural response induced by short-time transient loadings and has been used extensively for predicting the response of various types of structures (reinforced concrete in particular) to blast loads. Eight-node hexahedron (brick) elements were used to represent the concrete matrix while 2-node truss elements were used to represent the steel reinforcement, as shown in Figure 6 for the wall in case V-1. The extent of the models includes the entire SDW panel with an additional stub (one thickness in width) along those sides which are attached to orthogonal structural walls to approximate the resistance provided by those walls. No attempt was made to model the frangible portions of the structure (wood framing, hollow clay tile, etc.) under the assumption that they do not contribute materially to the response of the SDW. A fixed boundary condition was applied along all the stubs, while spatially varying pressure loads were applied over the inner surface of the SDW. Gravity loads were not included in these analyses as they tend to be overshadowed in their effects by the blast loading.

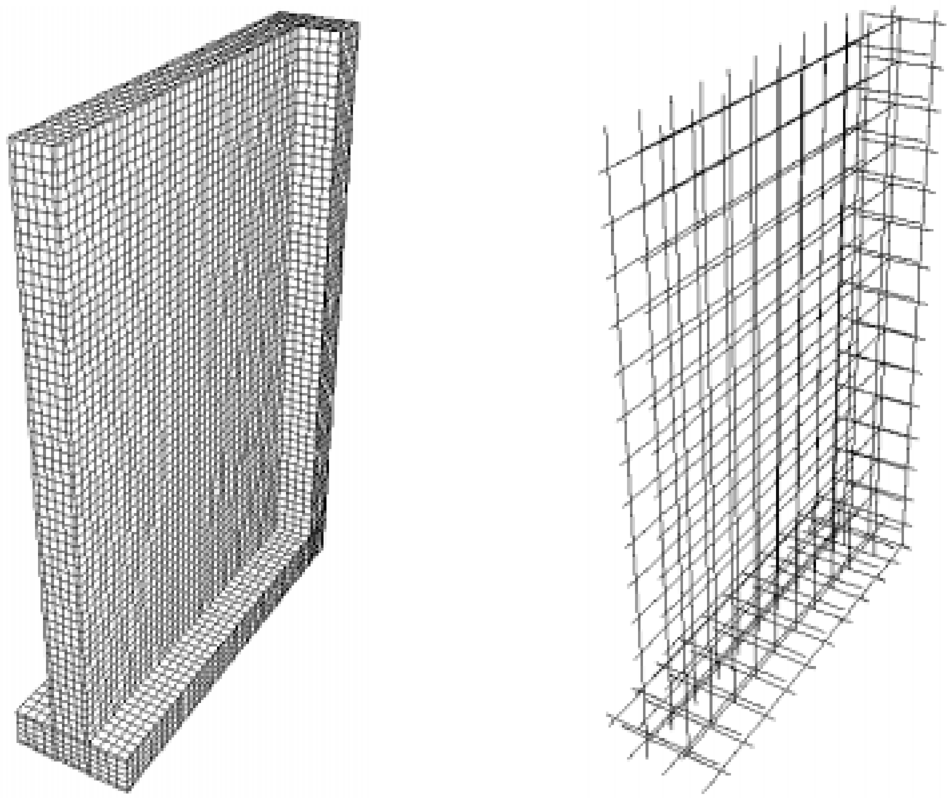

(a) Hexahedron elements for concrete. *(b) Truss elements for rebar.*

Figure 6. Finite element mesh used for validation case V-1.

The material model used to represent the concrete is based on a three-invariant formulation that was developed by Karagozian & Case over the past several years particularly for DYNA3D [5]. The constitutive model includes a number of state-of-the-art features that attempt to capture concrete's unique behavior: shear dilation (the volumetric expansion of concrete as it fails in shear), three failure surfaces (one each for the initial yield, maximum stress, and residual stress states), post-maximum stress ductility (instead of brittle fracture), and enhancement of strength as a function of strain rate. A rate dependent elastic-plastic model with strain hardening and rupture was used to represent the steel reinforcement.

This particular analytical methodology has been subject to extensive verification and validation efforts model and has been utilized to generate pre- and post-test results on a number of small- and large-scale experiments on hardened reinforced concrete structures. The concrete model was benchmarked against laboratory test results on small samples using simple, single- and multi-element models subjected to a wide variety of uniaxial, biaxial, and triaxial stress paths. An earlier study [6] correlated predicted debris velocities from SDWs exposed to high intensity blast loads to experimental data. More recently, the same methodology was used to generate analytical results for a number of reinforced concrete interior wall slabs exposed to internal blast loads, with very good correlation between the calculated and experimental data [7]. Thus, the methodology is considered to be relatively reliable, within reasonable uncertainty bounds.

LOADING MODEL

Computation of blast loads for the validation cases utilized the SHOCK [8] and FRANG [9] computer programs. The former computes spatially varying shock loads (peak pressures and total impulse) over the surface of the wall panel, while the latter calculates the gas pressure history in the room, which is assumed to be spatially uniform. The standard approach to combining the gas and shock pressure waveforms is illustrated in Figure 7. The triangular pulses from SHOCK and FRANG (both assumed to have instantaneous rise time and to arrive coincidentally) are overlaid and the outer envelope of the two is used to obtain the load; this is done over a 33 by 33 grid of target points, each with a unique SHOCK triangle but all of them using the same FRANG triangle. Note that the phasing of the load over the wall was not properly represented, as all loads are applied simultaneously at t=0.

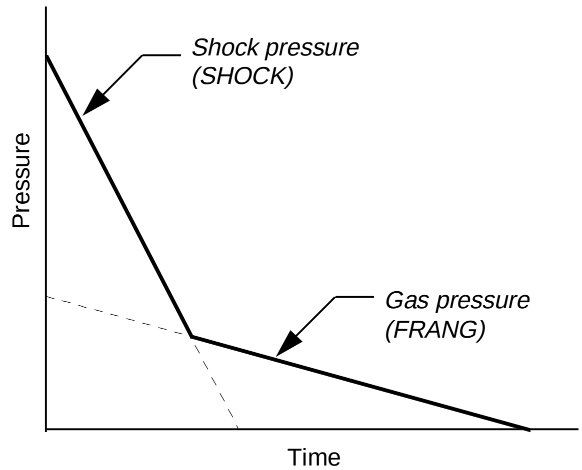

Figure 7. Method used to combine gas and shock loadings.

Since, as will be demonstrated below, the structural response is primarily sensitive to the gas phase of the loading, some additional detail is needed on how the gas pressures are computed by FRANG. Gas pressure is assumed to have an instantaneous rise to a peak level (computed as a function of the room volume and charge weight using standard curves), then decays gradually as a function of the vent area which in turn varies with time. FRANG uses the concept of covered and uncovered openings to define the venting conditions. Uncovered openings are those with no substantial covering and their vent area is fully available from the beginning. Covered openings are those which have a frangible cover such as wood framing, hollow clay tile, etc.; these are not expected to survive the effects of the blast but are assumed to be sufficiently massive to confine the expanding gases for some time. The mass per area of the covering is input by the user, and the code applies the pressure to that mass and computes its acceleration outward. The panel is assumed to remain integral as one piece as it displaces away from the cubicle, and the time-dependent vent area is computed by multiplying the perimeter of the opening by its displacement. The user is also able to input a panel recess depth which, if present, requires the panel to displace a certain distance before any vent area begins to accumulate.

Consequently, there is significant subjectivity in deciding precisely how to represent a given configuration within FRANG. The accepted standard methodology is the most conservative in that it results in the longest vent time and hence the greatest amount of impulse. For the configuration of case V-1, the roof was assumed to be a covered vent with a recess depth of 3 ft, so that the panel must translate 3 ft before any venting can occur. The frangible side wall, however, is not counted as an opening because it opens into a relatively confined corridor, with the assumption that the corridor will confine the gases and not serve as a vent. Because of these assumptions, the resulting gas pressure duration is very long and the impulse very high.

However, when initial structural response calculations using these loads showed complete failure of the SDW in V-1, two other gas pressure histories were also computed using different and less conservative assumptions; these affected only the duration of the pulse, not its magnitude. For load variation 2, the door in the front wall was represented as an uncovered vent, say, 4 ft by 7 ft = 28 sf; this number was arbitrarily increased to 40 sf to account for the frangibility of the front wall. Also, the assumed roof weight was lowered from 15 to 10 psf, but the other assumptions (area, perimeter, recess depth) were left unchanged. Load variation 3 represents an extreme case with the least conservative set of assumptions, wherein the entire roof and front wall are represented with uncovered vents and no covered vents are used whatsoever. In terms of the total impulse, variation 2 represents a midpoint between the extremes of variations 1 and 3. Key input and output parameters are summarized in Table 1.

Table 1. Assumptions for FRANG for validation case V-1.

Load Variation	**1**	**2**	**3**
INPUT			
Charge Weight	8.0	8.0	8.0
Volume of Room, ft^3	898	898	898
Covered Vent Area, ft^2	71	71	0
Vent Perimeter Around Panel, ft	34	34	0
Weight of Frangible Panel, psf	15	10	0
Shock Impulse on Frangible Panel, psi-ms	193	193	0
Uncovered Vent Area, ft^2	0	40	176
Recessed Depth of Panel, ft	3.0	3.0	0
OUTPUT			
Peak Gas Pressure, psi	84.6	84.6	84.6
Total Impulse, psi-ms	1810	820	110
Triangular Pulse Duration, ms	42.7	19.4	2.6

A comparison of the gas pressure histories output by FRANG is shown in Figure 8 (even though the actual analyses used an equivalent triangular pulse). For the prescribed methodology used in variation 1, we note that the roof panel takes a good 15 ms to clear the 3 ft recess depth, during which time there is no decay at all and lots of impulse is generated. The effect of adding uncovered vent area in load variation 2 is seen in that the decay begins from time zero; the clearing of the 3-foot recess is also clearly visible in the curve, as after that time the rate of decay is higher due to the greater vent area available. Finally, the most highly vented case of all (load variation 3) is seen to decay to zero in only about 5 ms. Figure 9 plots the three equivalent gas pressure triangles against the averaged shock pressure over the entire wall panel. We note that the shock pressure is much higher in magnitude, but the durations in load variations 1 and 2 are significantly longer for the gas pressure. Similarly, the majority of the impulse in the loads for variations 1 and 2 is derived from the gas pressure, not the shock pressure (compare the impulse values in Tables 3 and 4). In load variation 3, of course, the gas pressure duration is lower and the shock impulse is actually greater than the gas.

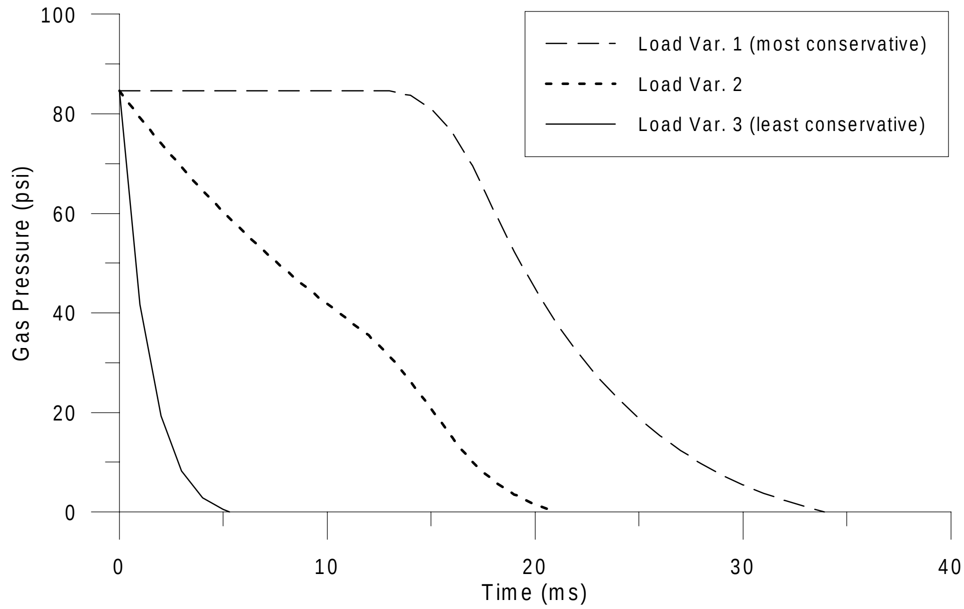

Figure 8. Comparison of gas pressures load variations for case V-1.

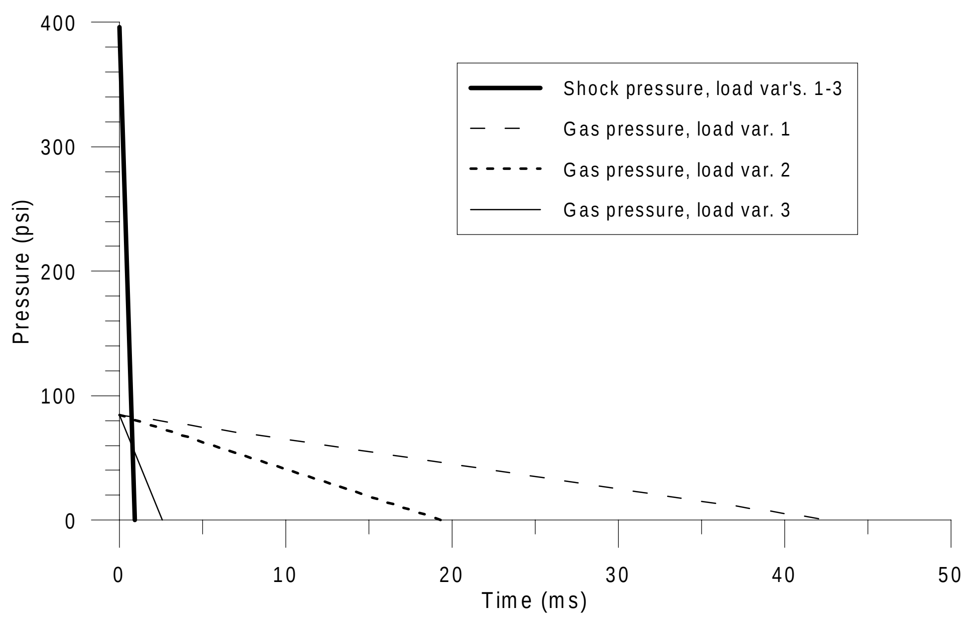

Figure 9. Comparison of average shock and gas loadings for case V-1.

ANALYSIS RESULTS

The three sets of loadings described above were applied to the finite element model of the SDW in case V-1 with, as might be expected, drastically different results. Histories of displacement at two key points along the wall's free edge (top corner and mid-height) are plotted in Figure 10. From these plots we see first that load variation 1 predicts complete and catastrophic failure of the wall: the peak displacement at the upper corner is near 70 inches by 80 msec and there is no indication that the velocities are beginning to turn around. By comparison, load variation 2 does reach a point of maximum displacement (nearly 70 inches at 250 msec), but the magnitude of deformation is so great that even if the model is stabilizing, failure would still be indicated due to the large deformations involved (e.g., through rebar pullout or lap splice failure). By comparison, load variation 3 predicts a very small level of deformation: only a peak of about 3½ inches at 50 msec. Compared to the 2-degree rotational criterion [2] of 6 inches, this is well below the design level and comparable to the deformations observed in the post-event photographs (Figure 2). It does, however, provide a reasonable lower bound to the response in light of the extremely high venting assumptions made to generate that particular set of loads. The suite of variations thus documents the range of responses that may be expected as a function of the variability in the assumptions made to generate the gas pressure loads. Note that the structure's long natural period of response (computed to be about 100 msec) makes the response heavily dependent on the total impulse delivered to the wall, rather than the peak pressures. Hence, since most of the impulse is bound up in the gas phase of the loading, the response is highly dependent on the assumptions made in generating that loading.

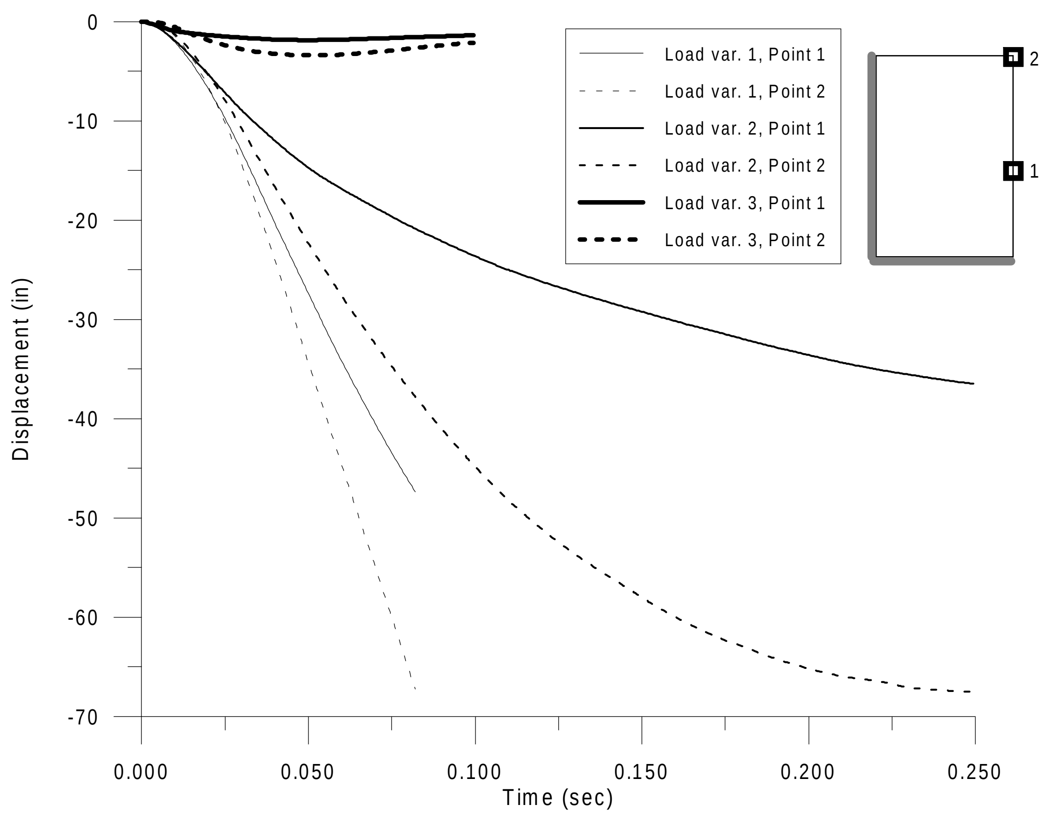

Figure 10. Displacement histories for validation case V-1.

But aside from the quantitative issue of the magnitude of response, its qualitative nature appears to have been mispredicted by the analytical model, regardless of the gas pressure assumptions. Figure 11 presents a series of deformed meshes, all without exaggeration, for the three loading variations. The point of maximum displacement is the free corner, as would be expected for a plate supported on two sides and loaded with a uniform. And in fact, while the shock component of the load is concentrated near the bottom of the wall, the dominance of the spatially uniform gas pressure over shock pressure, particularly in terms of impulse, makes the overall load effectively spatially uniform.

Figure 11 also shows fringes of maximum principal strain using a consistent colored gradation for the magnitude: blue is 0% while red is 60%. In load variation 1, the regions of strain concentration are primarily along the floor joint as well as along the vertical wall joint. The very high magnitudes of strain are indicative that the rupture strain of the reinforcing (around 15%) has been exceeded and some bars have broken. The areas of breakage are those away from the inner corner: near the top along the vertical joint, and near the outer edge along the horizontal joint. By comparison to variation 1, variation 2 predicts roughly similar strains along the vertical joint while the strains along the floor are much lower, low enough that bar failure is not indicated. For load variation 3, the maximum strains are only 4% and are not visible at this scale.

Comparing these results to the observed damage (Figures 2 and 3), we first recall that the actual wall deformation was bowed horizontally, with the greatest displacement in the middle; there was little apparent vertical gradient of displacement. By contrast, the models uniformly predict global rotation with the point of greatest displacement occurring at the unsupported corner, and with relatively equal displacement gradients in each of the two in-plane directions. Second, while failure of rebar is predicted for the most severe of the loading assumptions, the location of the failure does not match the observed result; i.e., the model predicts failures along the floor, while the actual event produced failures along the wall. Even for load variation 2 which predicted greater strains along the vertical joint, the region of maximum strain was near the top of the wall, unlike the observed damage which was localized in the lower 2/3 of the joint. These discrepancies may be explained by the fact that the model effectively ignored the top 3 feet of the wall (the portion projecting above the roof line). Since this portion would not receive the full shock and gas loads, its inertia and connection to the back wall would serve to reduce the predicted wall displacements and would help localize damage in the lower portions of the wall. Third, the standard loading methodology produced a result that indicated complete and catastrophic failure of the wall, whereas the actual wall simply deflected a few inches and remained upright.

Further consideration of the observed damage suggests that the actual location of the detonation was closer to the left side of the room, since the left side wall is much more damaged than the right. An explosion located only 2 or 3 feet away from the left side wall would deliver a much higher level of shock loading than the centered blast assumed in the calculations. This type of higher intensity, more spatially concentrated load is more in keeping with the observations of localized failure in the central-lower portion of the vertical joint. Furthermore, we would expect the gas pressure idealizations of instant rise time and spatial uniformity to not be fully realistic, causing further concentration of pressure near the explosive source. Still, the absence of the global rotation modes seen in the analyses does indicate that the large magnitude, spatially invariant, long duration gas pressures predicted by FRANG did not materialize.

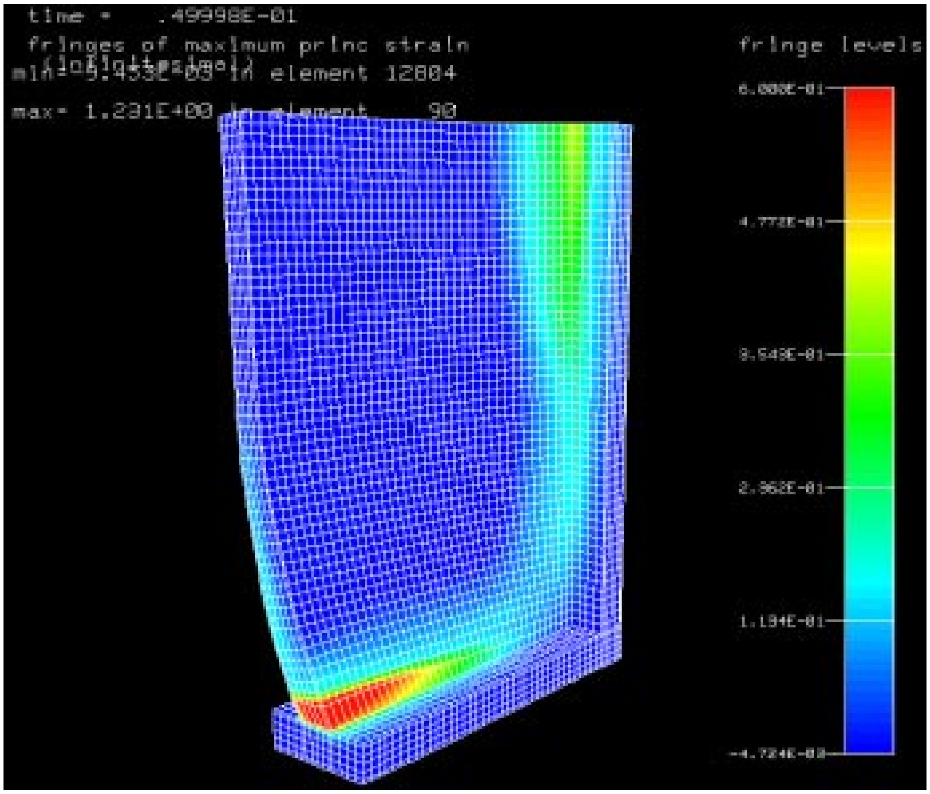

(a) Load var. 1, t= 50 ms

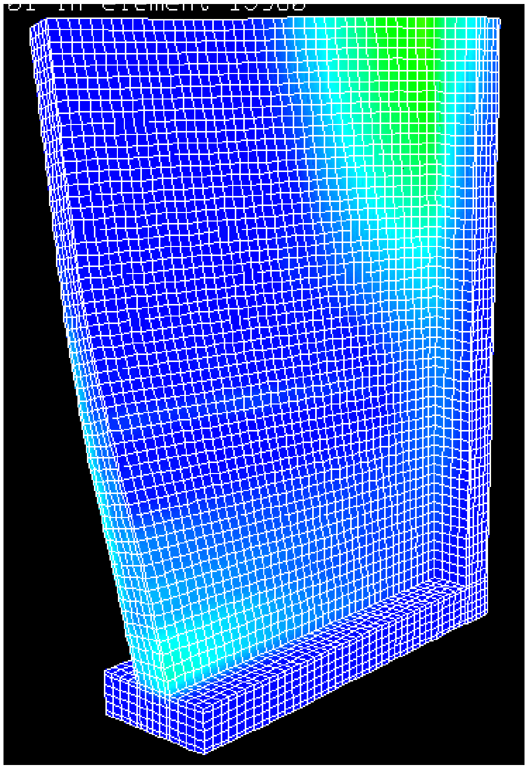

(b) Load var. 2, t=100 ms.

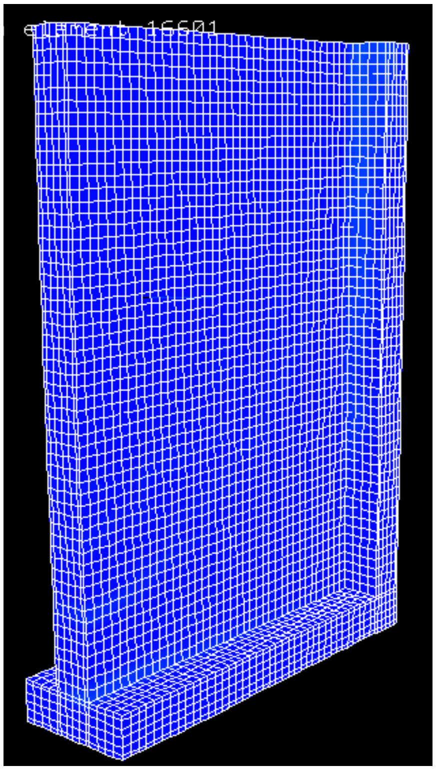

(c) Load var. 3, t=50 ms.

Figure 11. Color fringes of maximum principal strain.

Without exercising all the same kinds of loading variations, a similar calculation was also performed for case V-2 using only the nominal gas pressure methodology (i.e., analogous to load variation 1 for case V-1). While this accident involved a larger amount of explosive than V-1, the room volume was also greater hence the peak gas pressure was similar; the more highly vented conditions, however, resulted in less than half the impulse as in V-1. Nevertheless, the response of the SDW, summarized in the displacement/velocity history shown in Figure 12 for the unsupported corner, is equally catastrophic and indicative of complete collapse. Yet the observed level of damage to the concrete SDWs is extremely light, as seen in Figure 4, further reinforcing the observations drawn earlier for case V-1. Here as before, the wall behaves as a uniformly loaded plate supported on two sides, the free corner incurring the greatest amount of deflection.

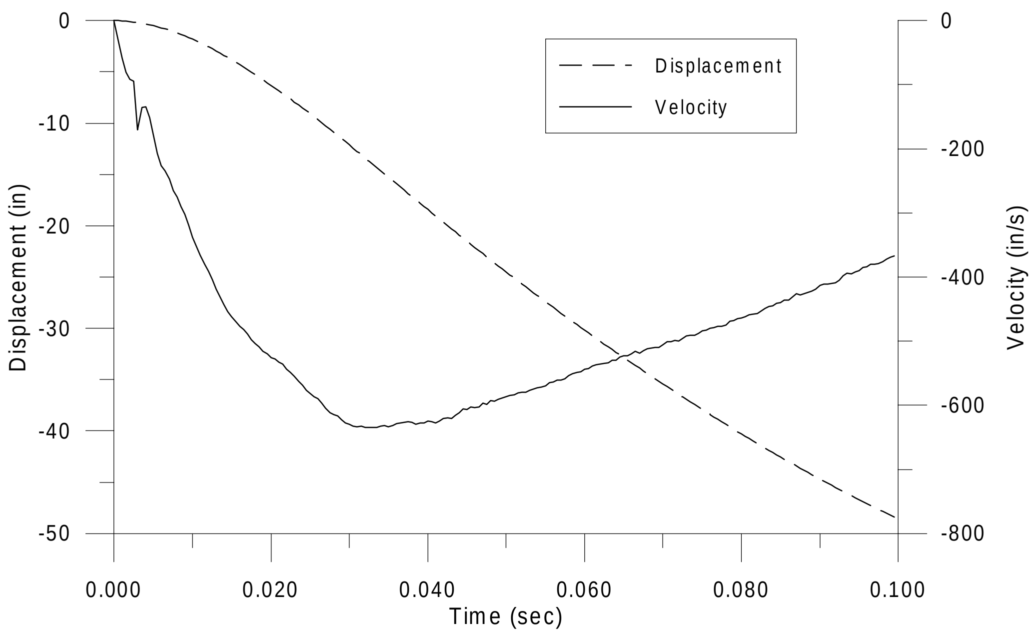

Figure 12. Velocity and displacement histories for validation case V-2.

CONCLUSIONS

Based on these results, a number of conclusions can be drawn regarding the accuracy and applicability of the methodology used to analyze the response of SDWs to blast loads:

- The calculated wall response is highly dependent on the gas phase of the loading, and in particular on the total impulse; hence, the response is very sensitive to variations in the assumptions made in deriving the gas pressure.

- The analysis consistently overpredicts wall response (by more than an order of magnitude) so long as the standard gas pressure derivation methodology is used.

- Due to the uncertainty in the gas portion of the load, there is a high level of uncertainty in the calculated responses; responses calculated using the standard load methodology should be regarded as very conservative upper bound estimates.

- The assumptions inherent to the standard load derivation methodology appear suspect, particularly the assumption of frangible panels remaining monolithic (*cf.* photographs of debris litter from cases V-1 & V-2), and the idealization of gas pressure being uniform and instantaneous over the entire wall surface (*cf.* bowed wall deformations in case V-1); more accurate loading models that represent the rise time and spatial distribution of gas pressure are needed in order to reduce the conservatism in the calculated wall response.

- The uncertainty and/or conservatism in the structural response model is overshadowed by that in the loading model; attempts to reduce conservatism should focus on assumptions in the gas pressure computations.

ACKNOWLEDGMENTS

The work reported in this paper was funded by the U. S. Army Industrial Operations Command, Safety Division, under the supervision of Mr. Jerry Bryan. The explosive accident data were obtained through the kind assistance of Dr. Chester Canada, DDESB. Technical supervision of the work was provided by the U. S. Army Engineering and Support Center, Huntsville.

REFERENCES

1. "DoD Ammunition and Explosives Safety Standards," DoD 6055.9-STD, Department of Defense Explosives Safety Board, Washington, D. C., July 1997.
2. "Structures to Resist the Effects of Accidental Explosions," Departments of the Army, the Navy, and the Air Force, Army TM 5-1300, Navy NAVFAC P-397, Air Force AFR 88-22, November 1990.
3. Bogosian, D. D., B. W. Dunn, and J. W. Wesevich, "An Analytical Investigation of the Blast Vulnerability of Substantial Dividing Walls," Karagozian & Case, Glendale, CA, TR-97-50.2, February 1998.
4. Whirley, R. G., "DYNA3D: A Nonlinear, Explicit, Three-Dimensional Finite Element Code for Solid and Structural Mechanics—User Manual," Lawrence Livermore National Laboratory (report UCRL-MA-107254), May 1991.
5. Malvar, L. J., J. E. Crawford, J. W. Wesevich, and D. Simons, "A New Concrete Material Model for DYNA3D, Release II: Shear Dilation and Directional Rate Enhancements," Karagozian & Case and Logicon RDA, K&C report no. TR-96-2.2, February 1996.
6. Bogosian, D. D., "Parametric Analysis of 12-Inch Substantial Dividing Walls," Karagozian & Case, Glendale, CA, TR-94-20, October 1994.
7. Wesevich, J. W., L. J. Malvar, and J. E. Crawford, "Comparison of Measured and Predicted Responses of Reinforced Concrete Walls Subjected to Close-in Blasts," *Proceedings of the 8th International Symposium on Interaction of the Effects of Munitions with Structures*, April 1997.
8. "SHOCK User's Manual, Version 1.0," Naval Civil Engineering Laboratory, Port Hueneme, CA, January 1988.
9. "FRANG User's Manual," Naval Civil Engineering Laboratory, Port Hueneme, CA, May 1989.